Thermal and Material Transfer in Turbulent Gas Streams: Local Transport from Spheres

N. T. HSU and B. H. SAGE

California Institute of Technology, Pasadena, California

Local convective thermal transfer is difficult to predict for nonuniform three-dimensional boundary flows. Direct measurements of local transfer from objects of practical interest are therefore useful in the prediction of thermal transfer and in an understanding of multi-dimensional boundary flows.

Measurements of the gross and local transfer were made upon a silver sphere 0.5 in. in diameter and a ceramic porous sphere of the same size from which *n*-heptane was permitted to evaporate. The air stream had a level of turbulence of approximately 5.4% and only small variation in velocity with position. Temperature distributions in the boundary flows around these spheres were determined, and from these distributions local transfer coefficients were established for the forward hemisphere. The gross transfers were established from the electrical energy added to the silver sphere and from the quantity of *n*-heptane evaporated from the porous sphere.

The local thermal transfers were in reasonable agreement with some of the theoretical analyses based upon a three-dimensional laminar-boundary layer. Satisfactory agreement was obtained between spatial integration of the local transfer and the simultaneously measured over-all values. These, in turn, were in fair agreement with correlated values of the gross thermal and material transfer from spheres.

The gross thermal transfer from spheres to fluids in fully developed turbulent flow has been well summarized by McAdams (*21*). Measurements for nearly potential flow were reported by Johnstone (*13*), and such transfers have also been studied by Tang (*31*). Significant differences in transfer resulting from the level of turbulence encountered in the air stream appear to exist. However, only limited experimental information has been available concerning the local transfer from spheres. Cary (*3*) reported experimental results for a 5-in. iron sphere in an air stream at Reynolds numbers between 4.4×10^4 to 1.5×10^5; no information as to the level of turbulence was available. Lautman and Droege (*16*) determined the local transfer from a 9-in. copper sphere in air at Reynolds numbers between 1.3×10^5 to 1.0×10^6. Xenakis and coworkers (*34*) repeated the work of Lautman and Droege in approximately the same range of Reynolds numbers, with a 9-in. sphere and with other spheres 6 and 12 in. in diameter. In these investigations a localized portion of the sphere was separately heated to the same temperature as the remainder of the sphere, and the energy transport from the localized portion to the air stream was determined as a function of angular position in the stream.

In the present study the rates of thermal transfer for 0.5-in. spheres with and without material transfer were determined at Reynolds numbers in a range of 1,530 to 4,200. The local thermal transport was established from the radial temperature gradients of the air stream

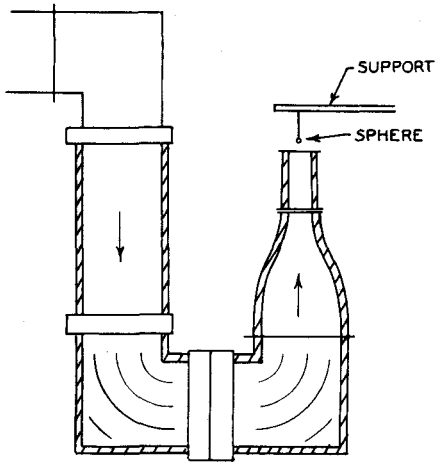

Fig. 1. Arrangement of air jet.

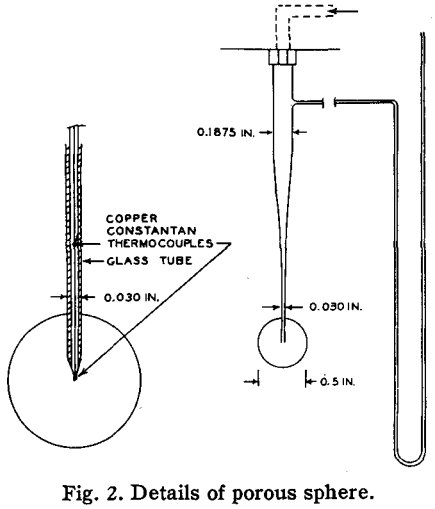

Fig. 2. Details of porous sphere.

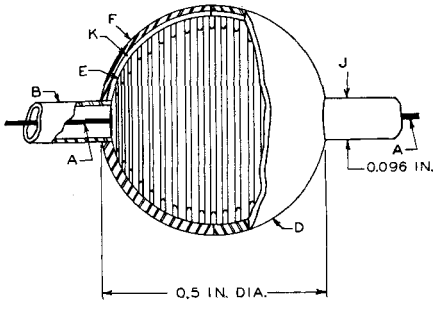

Fig. 3. Details of heated sphere.

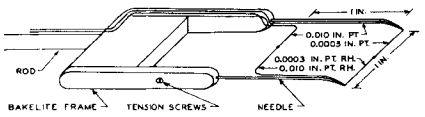

Fig. 4. Traversing thermocouple.

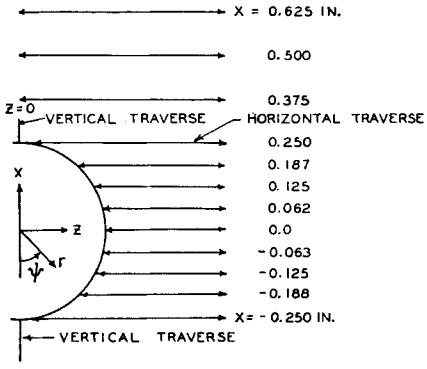

Fig. 5. Location of thermocouple traverses.

immediately adjacent to the sphere. This study constitutes a portion of a more general investigation of the influence of the level and scale of turbulence upon thermal and material transport.

ANALYSIS

The analysis of local thermal transfer for bodies immersed in a flowing stream is based upon a solution of the equation of motion of the boundary flows and the conservation of energy. Such work was carried out by Sibulkin (*29*), who presented an exact solution of thermal transfer at the stagnation point of the sphere for an incompressible fluid of constant intensive properties. The work of Sibulkin is based upon the equation of continuity, as well as upon the conservation of momentum and energy which apply to an incompressible fluid of constant heat capacity:

$$\frac{\partial(\sigma u)}{\partial s} + \frac{\partial(\sigma v)}{\partial n} = 0 \qquad (1)$$

$$u\frac{\partial u}{\partial s} + v\frac{\partial u}{\partial n} = u_1\frac{du_1}{ds} + \nu\frac{\partial^2 u}{\partial n^2} \qquad (2)$$

$$u\frac{\partial t}{\partial s} + v\frac{\partial t}{\partial n} = \mathrm{K}\frac{\partial^2 t}{\partial n_2} \qquad (3)$$

Equation (3) assumes a constant heat capacity for the air stream which permits a simple relationship between enthalpy and temperature. The boundary conditions for this situation are as follows:

$$n = 0 \quad : u = 0\,, \quad v = 0, \quad t = t_i$$

$$n = \infty \quad : u = u_1, \quad t = t_\infty$$

The local thermal flux at the surface of the sphere is established from

$$\overset{\circ}{q}_n = -k_i\left(\frac{\partial t}{\partial n}\right)_{n=0} \qquad (4)$$

The velocity distributions in a boundary layer about a sphere were established by Homann (*10*) by assuming a linear velocity profile with respect to distance along the surface of the sphere from stagnation.

Much effort has been directed (*7, 8, 15, 30*) to the application of the Kármán-Pohlhausen integral method (*14*) to include the prediction of the temperature distribution in the boundary layer of a sphere. Under the approximations of this method the following integral equations are obtained for the conservation of momentum and energy:

$$\frac{\partial}{\partial s}\int_0^{\delta_M} u^2\,dn - u_1\frac{\partial}{\partial s}\int_0^{\delta_M} u\,dn - \frac{1}{z}\frac{\partial z}{\partial s}\left(u_1\int_0^{\delta_M} u\,dn - \int_0^{\delta_M} u^2\,dn\right) = \delta_M u_1\frac{du_1}{ds} - \nu\left(\frac{\partial u}{\partial n}\right)_{n=0} \qquad (5)$$

$$\frac{\partial}{\partial s}\int_0^{\delta_t} u(t - t_\infty)\,dn + \frac{1}{z}\frac{\partial z}{\partial s}\int_0^{\delta_t} u(t - t_\infty)\,dn = -\mathrm{K}\left(\frac{\partial t}{\partial n}\right)_{n=0} \qquad (6)$$

In these expressions δ_M is the momentum-boundary-layer thickness and δ_t the thermal-boundary-layer thickness. The approximations of the Kármán-Pohlhausen analysis lead to the relation shown in Equation (7).

$$\frac{u}{u_1} = \phi_1\left(\frac{n}{\delta_M}\right) \qquad (7)$$

From this expression it follows that the temperature of the boundary layer may be related to the temperature of the main stream and of the surface of the sphere in the following way:

$$\frac{t - t_\infty}{t_i - t_\infty} = \Upsilon = \phi_2\left(\frac{n}{\delta_t}\right) \qquad (8)$$

Coefficients of the polynomial functions ϕ_1 and ϕ_2 may be established for the appropriate boundary conditions.

Korobkin (*15*) reported results from his studies in which he computed the local thermal transfer at the stagnation point by the integral method using Tomotika's distribution (*32*) for the temperature and velocity in the boundary layer of a sphere. Korobkin (*15*) included unpublished results of Sibulkin, who also calculated the local thermal transfer associated with the forward half of the sphere by integral methods.

Eckert (*8*) and Drake (*7*) submitted approximate methods for determining the local thermal transfer on a surface of revolution. Eckert's work yielded an exact solution to the energy equation for an incompressible laminar boundary layer over a wedge-shaped body. An approximate expression for the local thermal transport on an axially symmetric body was given by Drake (*7*), who applied the Mangler transformation (*20*) to the solution of this problem.

The foregoing analyses are based on the assumption that the radial velocity at the surface of the sphere can be taken as zero. In the case of evaporation from the surface of a sphere there usually exists a small hydrodynamic radial velocity at the surface. The solutions for boundary flows over a flat plate for situations with a velocity normal to the boundary have been obtained by Schlichting and Bussmann (*27*). Mickley and coworkers (*22*) extended these solutions by similarity considerations to the prediction of both thermal and material transfer. Spalding (*30*) established similar relationships for material transfer at the stagnation point of a sphere.

Under the conditions encountered in the present experimental investigations the normal velocity at the surface was not more than 0.005 ft./sec., as compared to a minimum stream velocity of 8 ft./sec. The composition of the gas phase at the surface of the porous sphere was always less than 0.05-mole fraction *n*-heptane. Under these conditions estimates based upon the results of the foregoing simplified analyses were used to establish the effect of material transfer on the temperature gradient.

Table 1. Decay of Longitudinal and Transverse Turbulence Behind Grid Used in Present Study

Distance downstream, in.	Gross velocity, ft./sec. 8 Longitudinal	8 Transverse	16 Longitudinal	16 Transverse
6	0.107*	0.085	0.100	0.082
9	0.075	0.064	0.072	0.062
12	0.059	0.054	0.056	0.050
13†	0.056	0.052	0.052	0.048
15	0.050	0.047	0.047	0.043

*Fluctuation velocity expressed as root-mean-square fraction of gross velocity.
†Downstream distance for present study.

METHODS AND EQUIPMENT

The present investigation involved measurement of the temperature distribution about a silver sphere and a porous sphere, each 0.5 in. in diameter. The sphere was located in an air stream at 100°F. and measurements were made at gross stream velocities of 8 and 16 ft./sec. The equipment employed to furnish the air supply has been described (*11*). The undisturbed stream had a level of turbulence of 0.013 as established by the methods of Schubauer (*28*). A perforated steel plate was used to create turbulence (*5*) and measurements were made with the sphere at a position 13 in. downstream from the plate. Some of the characteristics of the turbulent flow of the

air stream as taken from the measurements of Davis (*5*) are presented in Table 1. The velocity of the air stream was determined from its temperature and the weight rate of flow, which was established by means of a calibrated Venturi meter and associated equipment.

The porous sphere was prepared from synthetic-ceramic filter material. The general arrangement is shown in Figures 1 and 2. Liquid was introduced to the sphere at a known rate (*24*) through a small glass tube as shown in Figure 2. Copper-constantan thermocouples 0.003 in. in diameter were located at the positions indicated. Figure 3 gives a sectional view of the silver sphere, construction details of which are available (*1*). A small electrical heater was wound within a spiral groove E and was surrounded by the hemispheres F and D. A groove in the shell F, which is shown at K, permitted thermocouples to be mounted on the exterior shell. The thermocouples were brought out through the tubes B and J alongside the supporting wire A. These thermocouples were used for control purposes in the current measurements.

The temperatures in the boundary flows around the sphere were measured with a platinum, platinum-rhodium thermocouple 0.0003 in. in diameter, illustrated in Figure 4. The thermocouple was mounted upon a conventional "bird" with the reference junction in the air stream at a distance about 1 in. from the sphere. Corrections to the indicated temperature were made to account for thermal flux along the thermocouple (*19*). The locations of the traverses made in the boundary flows about the sphere are shown in Figure 5.

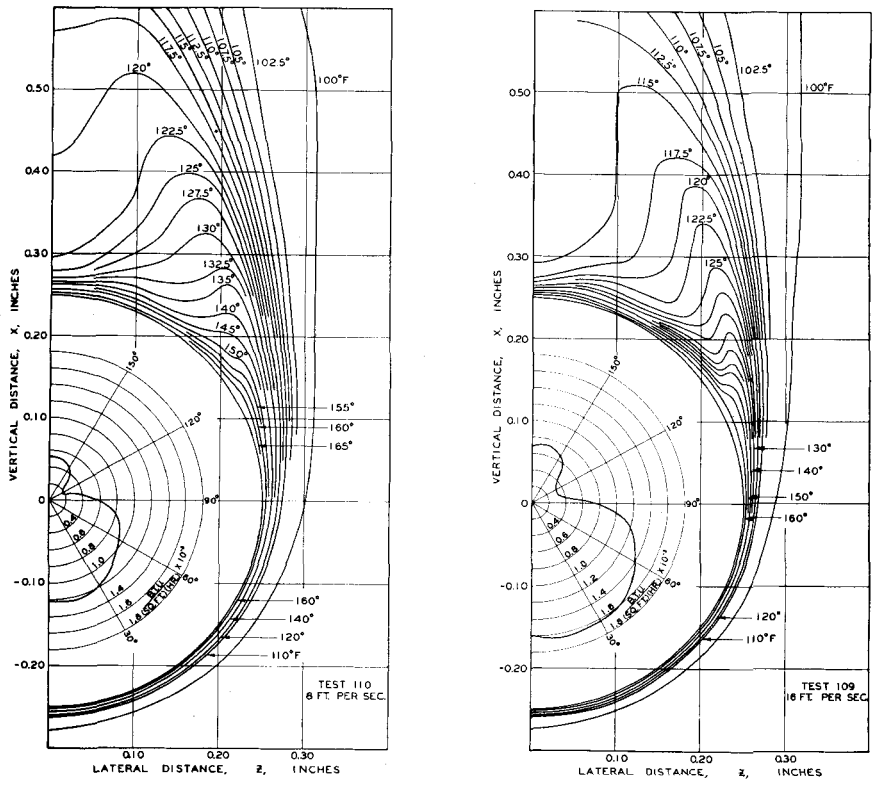

Fig. 6. Temperature distribution and local thermal flux around silver sphere.

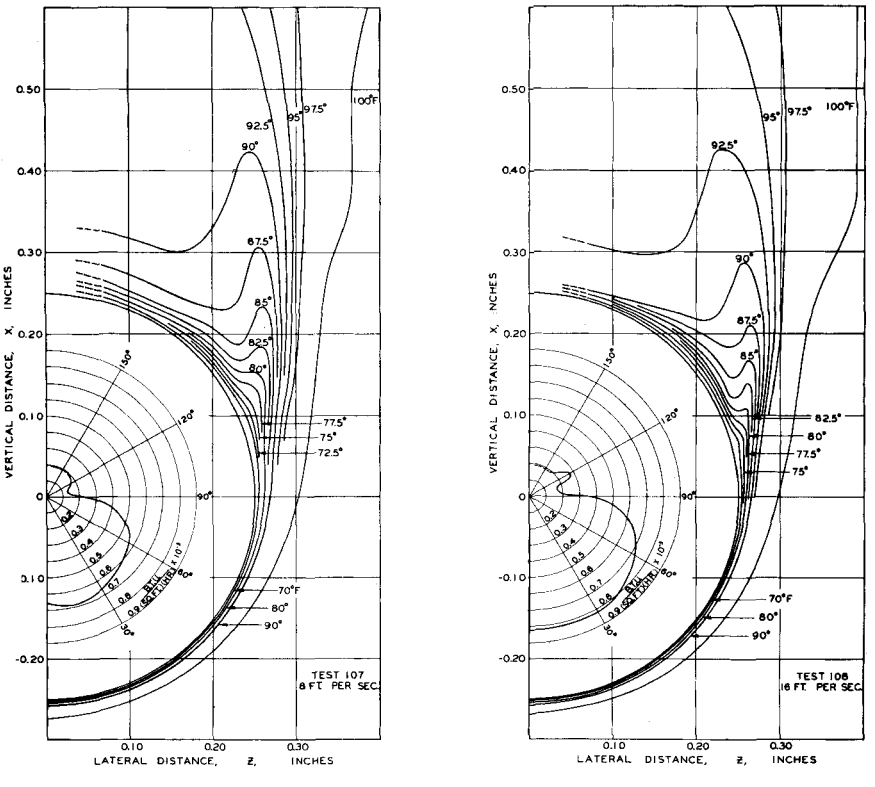

Fig. 7. Temperature distribution and local thermal flux around porous sphere.

MATERIALS

The properties of air and n-heptane employed in this investigation are available (*12*): the properties of air are based in part upon a set of critically chosen values (*23*), and thermal conductivity of n-heptane in the liquid phase was taken from McAdams (*21*). The effect of water and n-heptane upon the thermal conductivity of the air was determined by the methods proposed by Hirschfelder (*9*) and Lindsay and Bromley (*18*), respectively. The enthalpy change upon vaporization and the isobaric heat capacity of liquid n-heptane were taken from the data of Rossini (*25*) and Douglas and coworkers (*6*), respectively. In the calculations associated with this study it was not nesessary to consider the equation of state of the fluids in detail and, aside from minor corrections for the behavior of n-heptane, it was assumed that perfect gas laws applied, that local equilibrium obtained on the surface of the porous sphere, and that mixtures of n-heptane and air followed the laws of ideal solution (*17*).

The n-heptane was obtained as research grade from Phillips Petroleum Company and was subjected to a single fractionation in a column containing sixteen glass plates. The center 90% fraction of the overhead was retained for use.

EXPERIMENTAL RESULTS

The detailed experimental conditions which obtained in the course of the four sets of measurements are recorded in Table 2. Only two bulk velocities, of approximately 8 and 16 ft./sec., were investigated. The longitudinal turbulence level (*5*) was approximately 5.6% at the lower velocity and 5.2% at the higher velocity. The Reynolds number based upon the gross velocity and the kinematic viscosity of the fluid at the interface varied between 1,530 and 4,200.

A sample of the temperature measurements involving two different traverses is shown in Table 3. The radial distance

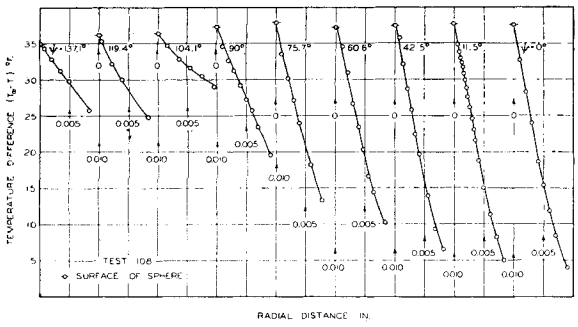

Fig. 8. Radial temperature distribution for test 108.

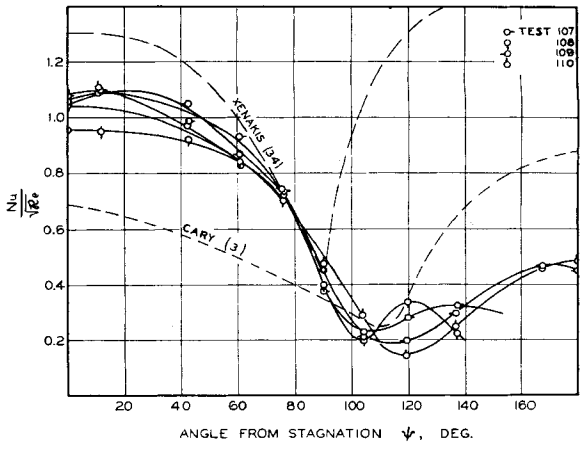

Fig. 9. Local experimental thermal transfer.

TABLE 2. EXPERIMENTAL CONDITIONS

Test number	107	108	109	110
Sphere				
Type	Porous	Porous	Silver	Silver
Diameter, in.	0.500	0.500	0.500	0.500
Total heptane evaporation rate $\times 10^6$, lb./sec.	3.878	5.515		
Total energy input $\times 10^3$, B.t.u./sec.			1.533	1.094
Average surface temperature, °F.	63.2	63.4	169.7	170.2
Temperature of liquid heptane entering sphere, °F.	96.9	97.9		
Air stream				
Bulk velocity, ft./sec.	8.04	16.23	16.13	8.06
Bulk temperature, °F.	100.1	100.1	100.1	100.1
Pressure, lb./sq. ft.	2,066.3	2,060.4	2,069.1	2,055.9
Weight fraction water	0.0065	0.0061	0.0030	0.0042
Turbulence level, %	5.6	5.2	5.2	5.6
Reynolds number, conditions at interface	2,100	4,200	3,060	1,530

from the center of the sphere as calculated from the traverse-position data is included, and the wire and the air temperatures are indicated. The details of all the experimental measurements are available (*12*). Results of the experimental investigations are summarized in Figures 6 and 7, which present the temperature distribution and local thermal flux around the silver and porous spheres for velocities of 8 and 16 ft./scc. The distribution of thermal flux at the surface of the sphere was evaluated by application of Equation (4) and is presented in polar coordinates in parts of Figures 6 and 7. An example of the radial temperature distribution for which the data of test 108 was utilized is shown in Figure 8. The radial temperature distribution shown was determined by appropriate graphical manipulations of the data of Figure 7.

The results for the local thermal transport at the surfaces of the spheres are available in tabular form (*12*). These data for local thermal transport at the surface of the spheres, as well as the average values of the data of Cary (*3*) and of Xenakis and coworkers (*34*), are presented in Figure 9. The standard deviation of the experimental points from the smooth curve is 0.0080 when it is assumed that all the error is in the Nusselt number. Cary's data covered the range of Reynolds numbers from 4.4×10^4 to 1.5×10^5, whereas the data of Xenakis were obtained at Reynolds numbers between 8.7×10^4 and 1.8×10^5. It is not clear what states were employed by Cary for evaluation of thermal conductivity and kinematic viscosity of the air stream. Xenakis used the temperature of the free stream for evaluation of these quantities. Korobkin (*15*) pointed out that Cary's data (*3*) may be low because of internal thermal exchange between the calorimeter and the remainder of the sphere. It is possible that the data of Xenakis were influenced by the position of the guy wires used in steadying the sphere in the wind tunnel.

Figure 10 which shows the average of the present experimental results in comparison with several theoretical investigations involving the work of Sibulkin (*29*), Eckert (*8*), Drake (*7*), and Korobkin (*15*), is limited to the forward hemisphere, for which several solutions of the boundary flow have been obtained. The present data are in fair agreement with the work of Eckert (*8*) and of Drake (*7*) and with the exact solution of Sibulkin (*29*) at stagnation. Current data yield

TABLE 3. SAMPLE OF TEMPERATURE MEASUREMENTS

Vertical traverse below sphere at $z = 0$ in. ($\psi = 0$ deg.)				Horizontal traverse at $x = -0.188$ in. ($\psi = 42.5$ deg.)			
Position x, in.	Wire temperature, °F.	Air temperature, °F.	Radius r, in.	Position z, in.	Wire temperature, °F.	Air temperature, °F.	Radius r, in.
−0.274	100.1	100.1	0.274	0.201	100.1	100.1	0.2752
−0.271	99.8	99.8	0.271	0.191	99.2	99.2	0.2680
−0.269	99.5	99.5	0.269	0.186	97.5	97.5	0.2645
−0.267	98.9	98.9	0.267	0.183	95.5	95.3	0.2624
−0.265	98.4	98.4	0.265	0.181	94.0	93.7	0.2610
−0.263	97.8	97.8	0.263	0.179	91.7	91.4	0.2596
−0.261	95.2	95.2	0.261	0.177	88.8	88.4	0.2582
−0.260	94.0	94.0	0.260	0.175	85.6	85.1	0.2568
−0.259	92.3	92.3	0.259	0.173	81.8	81.3	0.2555
−0.258	90.5	90.3	0.258	0.171	77.3	76.6	0.2541
−0.257	88.5	87.8	0.257	0.169	72.6	71.6	0.2528
−0.256	86.2	85.3	0.256	0.168	70.5	69.6	0.2521
−0.255	83.5	82.5	0.255	0.167	68.4	67.5	0.2515
−0.254	80.6	79.6	0.254	0.166	66.9	65.8	0.2508
−0.253	77.6	76.7	0.253	0.165*	63.0	61.5	0.2500
−0.252	74.4	73.3	0.252				
−0.251	70.5	69.1	0.251				
−0.250*	63.6	61.6	0.250				

*Indicates surface point.

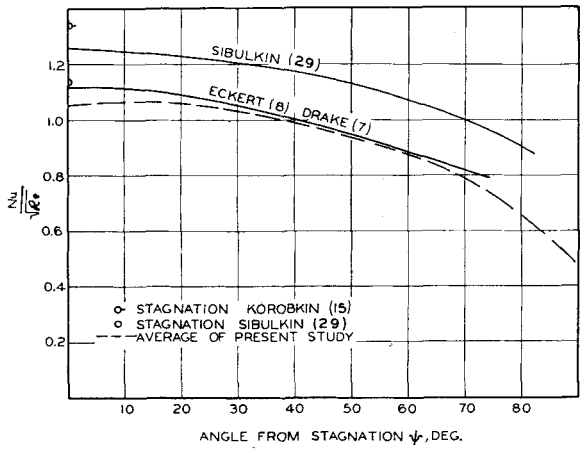

Fig. 10. Comparison of experimental and predicted local thermal transfer.

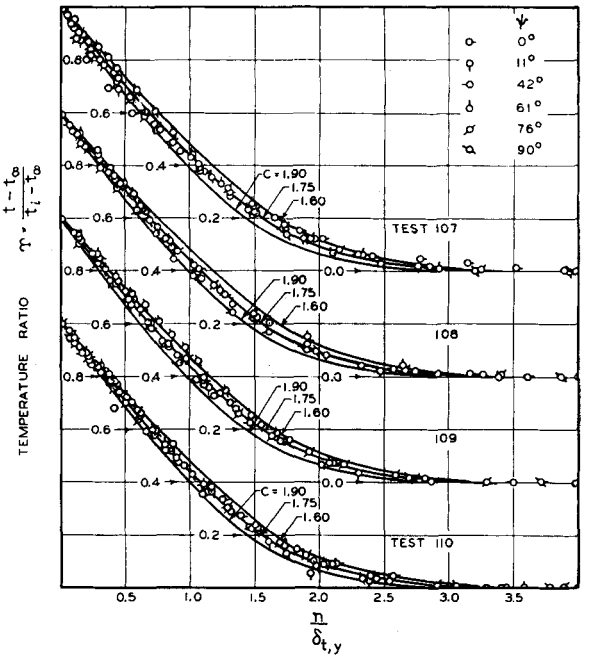

Fig. 11. Temperature distribution in boundary flow.

smaller values of local thermal transfer for conditions in the wake than were obtained from the experimental measurements of Xenakis (*34*) and Cary (*3*). The data of Cary (*3*) are closer to the current measurements than those of Xenakis (*34*). A larger uncertainty exists in the local thermal transfer in the wake as established from the current measurements than in the forward hemisphere.

Temperature distributions in the thermal boundary layer for the four investigations are recorded in Figure 11. The relationships between momentum and thermal boundary layers were established by assuming that the temperature ratio may be evaluated from

$$\Upsilon = 1 - f'\left(\frac{n}{\delta_{t,y}}\right) \qquad (9)$$

The displacement thickness of the thermal boundary layer was established from

$$\delta_{t,y} = \int_0^\infty \Upsilon \, dn \qquad (10)$$

The following empirical expression, which is based on the Blasius (*2*) function for a two-dimensional boundary flow, is included for comparison:

$$\Upsilon = 1 - f'\left(\frac{\eta}{c}\right) \qquad (11)$$

The behavior for varying values of the coefficient C is shown in Figure 11. The function f' was developed by Blasius (*2*), and numerical values are available (*4*). It is apparent that most of the current data satisfy Equation (11) for values of coefficient C varying between 1.60 and 1.90, with a probable value of C of 1.75. The assumptions underlying the derivation of Equation (11) are such as to make the detailed applicability of such a simple treatment uncertain.

Figure 11 illustrates the relatively narrow range of temperature distribution encountered for all positions and conditions of flow and transport. A detailed and exact analysis of the local thermal transfer to spheres awaits a satisfactory analysis of the three-dimensional boundary flow associated with the motion of a gas of varying properties around a spherical surface. No effect of the level of turbulence has been considered in available analyses.

The arrangement of the supports for the silver sphere made undesirable the integration of the local thermal transport for comparison with the gross transport established from the measured electrical power. As yet unpublished experimental data gathered from tests made with a larger silver sphere supported by a single tube in the aft hemisphere led the authors to believe that uncertainties of the order of 1% may be involved. The presence of the tubes at the equator results in an increase in the gross thermal transport (*26*). In the case of the porous sphere, calculations of the total thermal transport appeared worth while. The total interfacial thermal flux determined from the local temperature gradients was established from

$$\mathring{Q} = -\oint_0^A k_i \left(\frac{\partial t}{\partial n}\right)_{n=0} dA \qquad (12)$$

In Equation (12) the scalar total thermal flux is considered positive when energy is transmitted in the direction of increasing coordinate n. The total interfacial thermal flux determined from an over-all energy balance may be established from the following equation:

$$\mathring{Q} = -\mathring{m}[L + C_{P,l}(t_g - t_l)] + (k_h A_h + k_t A_t + k_w A_w)\left(\frac{\partial t}{\partial x}\right)_{n=0} - \mathring{Q}_r \qquad (13)$$

In Equation (13) the vectorial nature of the transport was taken into account when signs were determined. The radiation correction in Equation (13) is given by

$$\mathring{Q}_r = A\beta(T_i^4 - T_{sr}^4)\frac{1}{\frac{1}{\epsilon_{sr}} + \frac{1}{\epsilon_{sp}} - 1} \qquad (14)$$

It was found, as shown in Table 4, that with an emissivity for wetted silica (*21*) of 0.8, reasonable agreement was obtained between the gross thermal transports from the porous sphere as established from Equations (12) and (13), respectively.

The gross thermal transport associated with the porous and silver spheres is presented in Figure 12 as a function of Reynolds number. The results of McAdams (*21*), based primarily upon data

Table 4. Comparison of Measured and Integrated Total Convective Transfer for Porous Sphere

Test	Enthalpy change	Thermal flux: Corrections, Conduction	Corrections, Radiation	Evaporation*	Temperature† gradient	Difference, %
107	0.544‡	−0.003	−0.033	0.508	0.519	−2.2
108	0.772	−0.003	−0.036	0.733	0.680	6.4

*Established from evaporation rate with Equation (10).
†Established from local temperature gradient at surface with Equation (9).
‡Values expressed in B.t.u./sec. × 10^{-3}; for example, first entry is 0.000544 B.t.u./sec.

of Williams (*33*), yield somewhat higher values of the thermal transfer than were obtained for the porous sphere; however, the data of Johnstone (*13*) are in good agreement with the current study. The information reported for low Reynolds numbers by Tang (*31*) is markedly below the present measurements.

The agreement between the data of other investigators and the present measurements as presented in Figure 12 is deemed satisfactory when the level of turbulence encountered in the present measurements is taken into account. It has been found that the level of turbulence introduces a rather marked influence on the convective transport particularly at Reynolds numbers above 4,000 (*26*).

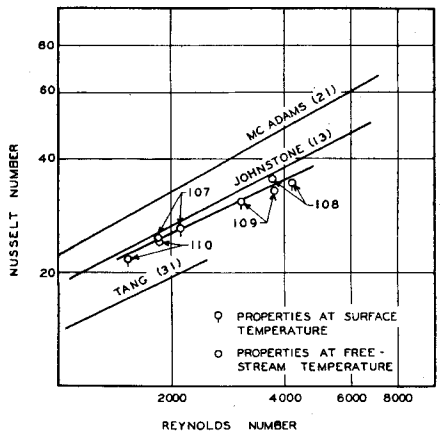

Fig. 12. Comparison of gross thermal transfer to spheres from several investigators.

ACKNOWLEDGMENT

The Fluor Corporation contributed to the support of the experimental program. N. T. Hsu was a Peter E. Fluor Fellow during the period in which these experimental data were obtained Kazuhiko Sato assisted with the experimental measurements, Betty Kendall and Virginia Berry contributed markedly to the reduction of the experimental data, and June Gray prepared the figures. W. N. Lacey reviewed the manuscript.

NOTATION

A = area, sq. ft.
C = constant
C_P = isobaric heat capacity, B.t.u./(lb.)(°F.)
D = diameter, ft.
d = differential operator
f' = Blasius function
h = thermal transfer coefficient, B.t.u./(sq. ft.)(sec.)(°F.)
k = thermal conductivity, B.t.u./(sq. ft.)(sec.)(°F./ft.)
L = latent heat of vaporization, B.t.u./lb.
$\dot{m}$ = total weight rate of transport from surface, lb./sec.
n = radial or normal distance from surface, in. or ft.
Nu = Nusselt number, hD/k_i
$\dot{Q}$ = gross rate of convective thermal transfer from surface, B.t.u./sec.
$\dot{Q}_r$ = gross rate of radiant transfer from surface, B.t.u./sec.
$\dot{q}_n$ = local thermal flux in direction n, B.t.u./(sq. ft.)(sec.)
r = radial distance from center of sphere, in. or ft.
Re = Reynolds number, DU/ν_i
s = distance parallel to surface in direction of main flow, ft.
T = thermodynamic temperature, °R.
t = temperature, °F.
U = bulk or free stream velocity, ft./sec.
u = local velocity along s, ft./sec.
u_1 = local velocity at the edge of momentum boundary layer, ft./sec.
v = local velocity along n, ft./sec.
x, z = coordinate axes with origin at center of sphere, in. or ft.

Greek Letters

β = Stefan-Boltzmann constant, 0.1713 $\times 10^{-8}$ B.t.u./(sq. ft.)(hr.)(°R.^{4})
δ_M = momentum-boundary-layer thickness, ft.
δ_t = thermal-boundary-layer thickness, ft.
$\delta_{t,v}$ = displacement thickness of thermal boundary layer, ft.
ϵ = emissivity
η = Blasius parameter
K = thermometric conductivity, sq. ft./sec.
ν = kinematic viscosity, sq. ft./sec.
σ = specific weight, lb./cu. ft.
τ = nondimensional temperature ratio, $(t - t_\infty)/(t_i - t_\infty)$
ϕ = function of
ψ = polar angle measured from the stagnation point, deg.
∂ = partial differential operator

Subscripts

g = gas phase
h = liquid n-heptane
l = liquid phase
i = interface
t = tube
sp = sphere
sr = surroundings
w = thermocouple wire
∞ = free stream condition

LITERATURE CITED

1. Baer, D. H., W. G. Schlinger, V. J. Berry, and B. H. Sage, *J. Appl. Mechanics*. **20**, 407 (1953).
2. Blasius, Heinrich, *Z. angew. Math. u. Phys.*, **56**, 1 (1908).
3. Cary, J. R., *Trans. Am. Soc. Mech. Engrs.*, **75**, 483 (1953).
4. Corcoran, W. H., J. B. Opfell, and B. H. Sage, "Momentum Transfer in Fluids," Academic Press, Inc., New York (1956).
5. Davis, Leo, *Rept.* 3-17, Jet Propulsion Laboratory, Calif. Inst. Technol. (1952).
6. Douglas, T. B., G. T. Furukawa, R. E. McCoskey, and A. F. Ball, *J. Research Nat'l. Bur. Standards*, **53**, 139 (1954).
7. Drake, R. M., Jr., *J. Aeronaut. Sci.*, **20**, 309 (1953).
8. Eckert, Ernst, *Forsch. Gebiete Ingenieurew., Forschungsheft* No. 416, p. 1 (1942).
9. Hirschfelder, J. O., R. B. Bird, and E. L. Spotz, *Trans. Am. Soc. Mech. Engrs.*, **71**, 921 (1949).
10. Homann, Fritz, *Z. angew. Math. u. Mech.*, **16**, 153 (1936).
11. Hsu, N. T., Kazuhiko Sato, and B. H. Sage, *Ind. Eng. Chem.*, **46**, 870 (1954).
12. Hsu, N. T., and B. H. Sage, Document 5311. Am. Doc. Inst., Washington 25, D. C.; $5.00 for photoprints or $2.25 for 35-mm. microfilm.
13. Johnstone, H. F., R. L. Pigford, and J. H. Chapin, *Trans. Am. Inst. Chem. Engrs.*, **37**, 95 (1941).
14. Kármán, Th. von, *Z. angew. Math. u. Mech.*, **1**, 244 (1921).
15. Korobkin, Irving, *Am. Soc. Mech. Engrs.*, Paper 54-F-18, Am. Soc. Mech. Engrs. Milwaukee Meeting (September 1954).
Milwaukee Meeting, (September 1954).
16. Lautman, L. G., and W. C. Droege, Serial No. AIRL A6118, Air Materiel Command, 50-15-3 (August, 1950).
17. Lewis, G. N., *J. Am. Chem. Soc.*, **30**, 668 (1908).
18. Lindsay, A. L., and L. A. Bromley, *Ind. Eng. Chem.*, **42**, 1508 (1950).
19. Longwell, P. A., W. W. Short, and B. H. Sage, submitted to *J. Appl. Phys.*
20. Mangler, W., *Z. angew. Math. u. Mech.*, **28**, 97 (1948).
21. McAdams, W. H., "Heat Transmission," McGraw-Hill Book Company, Inc., New York (1954).
22. Mickley, H. S., R. C. Ross, A. L. Squyers, and W. E. Stewart, *Natl. Advisory Comm. Aeronaut., Tech. Note* 3208 (July 1954).
23. Page, Franklin, Jr., W. H. Corcoran, W. G. Schlinger, and B. H. Sage, Doc. 3293, Am. Doc. Inst., Washington, D. C. (1951).
24. Reamer, H. H., and B. H. Sage, *Rev. Sci. Instr.*, **24**, 362 (1953).
25. Rossini, F. D., et al., "Selected Values of Physical and Thermodynamic Properties of Hydrocarbons and Related Compounds," Carnegie Press, Pittsburgh (1953).
26. Sato, Kazuhito, and B. H. Sage, *Trans. Am. Soc. Mech. Engrs.* (to be published).
27. Schlichting, Hermann, and K. Bussmann, *Schriften. deut. Akad. Luftfahrtforsch.*, **7B**, Heft 2 (1943).
28. Schubauer, G. B., *Natl. Advisory Comm. Aeronaut. Tech. Rept.* 524 (1935).
29. Sibulkin, Merwin, *J. Aeronaut. Sci.*, **19**, 570 (1952).
30. Spalding, D. B., *Proc. Roy. Soc. (London)*, **A221**, 78 (1954).
31. Tang, Y. S., J. M. Duncan, and H. E. Schweyer, *Natl. Advisory Comm. Aeronaut., Tech. Note* 2867 (March, 1953).
32. Tomotika, S., *Aeronaut. Research Comm. Reports* and *Mem.* 1678 (July 1935) (England).
33. Williams, G. C., Sc.D. thesis, Massachusetts Inst. Technol., Cambridge (1942).
34. Xenakis, G., A. E. Amerman, and R. W. Michelson, *WADC Tech. Rept.* 53-117, Wright Air Development Center, Dayton, Ohio (April, 1953).